Solitary structures associated with Short Large-Amplitude Magnetic Structures (SLAMS) upstream of the Earth's quasi-parallel bow shock

R. Behlke[1,2], M. André[1], S.D. Bale[3], J.S. Pickett[4], C.A. Cattell[5], E.A. Lucek[6], and A. Balogh[6]

For the first time, solitary waves (SWs) have been observed within Short Large-Amplitude Magnetic Structures (SLAMS) upstream of the Earth's quasi-parallel bow shock. The SWs often occur as bipolar (at times tripolar) pulses in the electric field data. Additionally, high-frequency wave packets around the electron gyro-frequency f_{ce} and the proton plasma frequency f_{pi} are found. The observed SWs move parallel to the background magnetic field at velocities of v = 400 - 1200 km/s. They have peak-to-peak amplitudes in the parallel electric field of up to $E'_{\|} = 65$ mV/m and parallel scale sizes of $L_{\|} \sim O(10)\ \lambda_D$. The bipolar solitary waves exhibit negative potential structures of $|\Phi_{\|}| = 0.4 - 2.2$ V, i.e., $e\Phi_{\|}/kT_e \sim O(0.1)$. None of the theories commonly used to describe SWs are well suited to identify these negative potential structures moving at velocities above the typical ion thermal speed in a weakly magnetized plasma.

1. Introduction

The character of collisionless shocks is determined by the angle θ_{Bn} between the upstream magnetic field and the nominal shock normal. At the Earth's quasi-parallel bow shock, so-called Short Large-Amplitude Magnetic Structures (SLAMS) are commonly observed (Schwartz et al., 1992; Lucek et al., 2002; Behlke et al., 2003). Observations combined with simulations (Burgess, 1989) led to the model of a cyclically reforming shock which is built up of a patchwork of SLAMS (Schwartz and Burgess, 1991). The quasi-parallel shock could thus be described as an extended transition region characterized by the growth, deceleration and merging of SLAMS rather than a single shock surface.

Solitary waves (SWs) travelling parallel to the background magnetic field have been reported from various parts of the magnetosphere. They are characterized by their bipolar electric field structure parallel to the magnetic field. SWs were first observed in the auroral acceleration region by S3-3 (Temerin et al., 1982). They are found at narrow boundaries, such as the plasma sheet boundary (Matsumoto et al., 1994; Cattell et al., 1998) and the quasi-perpendicular bow shock (Bale et al., 2002) and in regions with strong currents, such as the auroral acceleration region (Mozer et al., 1997). Observations of SWs were also reported from the solar wind (Mangeney et al., 1999), the magnetosheath (Pickett et al., 2003), at high-altitude cusp injections (Cattell et al., 2001) and the magnetopause (Cattell et al., 2002). In most cases, the structures were identified as electron solitary waves. They are observed at both high and low altitudes for a wide range of $f_{\rm ce}/f_{\rm pe}$. However, ion solitary waves have so far only been reported from the low altitude auroral region where $f_{\rm ce}/f_{\rm pe} \gg 1$ (Boström et al., 1988; Bounds et al., 1999; Crumley et al., 2001; Dombeck et al., 2001; McFadden et al., 2003). In this letter, we present the first observations, as known to the authors, of solitary structures within SLAMS.

The data for this study were obtained by the Electric Field and Wave (EFW) experiment (Gustafsson et al., 1997) onboard the four Cluster spacecraft (Escoubet et al., 1997). The EFW experiment consists of two pairs of spherical probes on wire booms in the spin plane of each satellite (approximately the ecliptic plane). The probe-to-spacecraft separation is 44 m. For the data presented here, the probe potential with respect to the spacecraft is sampled both at 9,000 samples per second (internal burst mode data rate, called IBM hereafter), as well as at 5 samples per second (normal mode data rate, called NM hereafter). This measurement is usually referred to as the negative of the spacecraft potential $-V_{sp}$ and gives an estimate of the plasma density (Pedersen et al., 2001). Furthermore, data from the fluxgate magnetometer (FGM), see Balogh et al. (2001), are used for the identification of SLAMS.

2. Observations

An example of a quasi-parallel bow shock crossing on February 3, 2002, at ~(12, 3, -8) R_E (in GSE) is presented in Figure 1. The transition from the solar wind (UT 04:30-04:50) to a more turbulent region (from UT 04:50) with magnetic field and density pulsations can clearly be seen in panels (a)-(b) which display $-V_{sp}$ and the magnetic field magnitude B, respectively. In panels (c)-(e), a shorter interval of 1 min (UT 04:59:20-05:00:20) reveals typical signatures of Short Large-Amplitude Magnetic Structures (SLAMS). During this interval, two SLAMS are observed at UT 04:59:35 and 04:59:42. They are characterized by density enhancements (Behlke et al., 2003), as seen in panel (c), as well as magnetic field enhancements (Schwartz et al., 1992), as seen in panel (d). SLAMS are typically associated with rotations of the magnetic field (Schwartz et al., 1992), see panel (e) which shows the magnetic field elevation θ_B. Note that θ_B is the elevation of the magnetic field

[1]Swedish Institute of Space Physics, Uppsala division, Uppsala, Sweden.
[2]Department of Astronomy and Space Physics, Uppsala University, Uppsala, Sweden.
[3]Space Sciences Laboratory, University of California, Berkeley, USA.
[4]Department of Physics and Astronomy, University of Iowa, Iowa City, USA.
[5]School of Physics and Astronomy, University of Minnesota, Minneapolis, USA.
[6]Blackett Laboratory, Imperial College, London, UK.

0094-8276/03/$5.00

over the spin plane of the spacecraft, whereas θ_{Bn}, as used in Sect. 1, is the angle between the upstream magnetic field and the shock normal. Although all four Cluster spacecraft were recording data during this period, we only present data for one spacecraft in this plot. Firstly, IBM data are only recorded for one satellite at a time. Secondly, the plot is restricted to one spacecraft for clarity reasons, since panels (c)-(e) are nearly identical during this event at $\sim$ 100 km separation between the satellite. For multi-spacecraft observations of SLAMS, see Lucek et al. (2002) and Behlke et al. (2003). A zoom-in of panel (c) is shown in panel (f) displaying an interval of 11.5 sec during which an internal burst was recorded. The black circles give the NM data whereas the red line shows the IBM data for probe 2.

Note that some features of the SLAMS are only visible in the IBM data. Firstly, the right-hand side of the SLAMS (i.e., the leading edge) around UT 04:59:35 appears much steeper in the IBM data than in the NM data, additionally exhibiting an over-shoot-like feature. Earlier observations of SLAMS with longer duration (around 15 sec) already revealed the feature of a steepened leading edge, but did not show over-shoot-like characteristics (Lucek et al., 2002; Behlke et al., 2003). Observations of quasi-perpendicular shock crossings commonly display an overshoot. Secondly, short-duration, high-amplitude spikes as well as high-frequency wave packets are observed in the IBM data. During this quasi-parallel shock crossing, two more IBM data sets have been recorded on other spacecraft adding up to 33 sec of high-resolution data.

Figure 2 shows two short intervals of 100 msec with IBM data for spacecraft 4. $E_{\|}$ and $E_{\perp}$ are defined as the electric

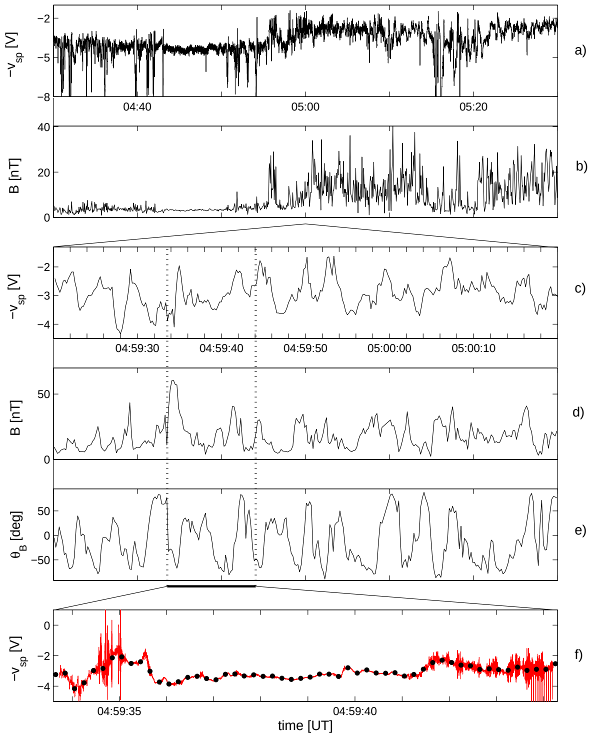

Figure 1. A quasi-parallel shock crossing observed by Cluster satellite 4 on February 3, 2002. Note the different time intervals for panels (a)-(b), (c)-(e) and (f), respectively. Panel (a) shows the negative spacecraft potential $-V_{sp}$ for UT 04:30-05:30. This parameter is correlated with the plasma density, i.e., high $-V_{sp}$ corresponds to a high density (e.g., a $-V_{sp}$ of -8, -5, -2 V corresponds to about 6, 20, 100 particles cm^{-3}). Panel (b) displays the magnetic field magnitude B from FGM for the same period. Panels (c)-(e) show 1 min of data (UT 04:59:20-05:00:20) of the negative spacecraft potential $-V_{sp}$, the magnetic field magnitude B and the elevation angle of the magnetic field θ_B, respectively. Here, $\theta_B = 90°$ corresponds to a strictly northward field. Panel (f) displays 11.5 sec of $-V_{sp}$ data (UT 04:59:33.6-04:59:45.1) for probe 2. The red line gives the IBM data (9 kHz sampling rate) with NM data (5 Hz sampling rate) overlayed as black circles. The pattern of vertical lines in panel (f) at 04:59:44 is due to the active sounding of the WHISPER instrument.

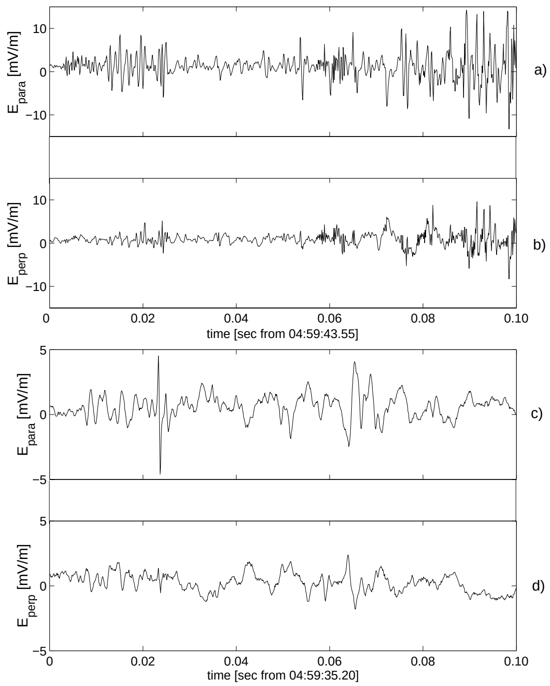

Figure 2. Observations by Cluster 4 on February 3, 2002. Panels (a)-(b) display $E_{\|}$ and $E_{\perp}$ (definition see text) with start at UT 04:59:35.9. Panels (c)-(d) give $E_{\|}$ and $E_{\perp}$ with start at UT 04:59:35.2.

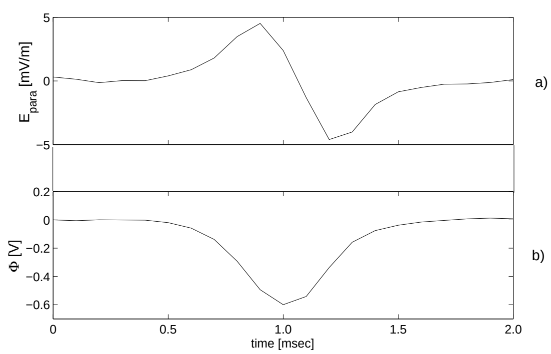

Figure 3. 2002-02-03, UT 04:59:35.22: Cluster observations of a solitary wave exhibiting the charateristic bipolar signature in the parallel electric field component (panel a). Panel (b) shows the potential over the structure with $\Phi_{\|} \approx$ -0.6 V.

field components in the spin plane of the spacecraft parallel and perpendicular to the ambient magnetic field, respectively (for $\theta_B \sim 0$). The solitary waves occur in groups (panels (a)-(b)) or as single structures (panels (c)-(d)). They have durations Δt less than or approximately 1 msec and peak-to-peak amplitudes in the parallel electric field $E'_{\parallel}$ of the order of or above 10 mV/m. Several spikes are embedded in a weaker irregular wave field.

Solitary waves (SWs) are in general, as well as in SLAMS, characterized by a bipolar electric field pulse parallel to the background magnetic field. To determine the physical structure of a SW, its velocity vector must be determined. This can be done using the four probes as an interferometer. The procedure is described in detail by Dombeck et al. (2001). This method returns scale sizes that are approximately four times larger than those obtained by a potential fit to a Gaussian (Cattell et al, 2003). The first method is based on the gradient in the parallel electric field change, whereas the latter method uses the Gaussian half-width. Panel (a) in Figure 3 shows a zoom-in of panel (c) in Figure 2. It displays the well-resolved parallel electric field component of a solitary structure. The analysis for this SW yields a velocity of $v \sim 400$ km/s. The potential depth as integrated over the parallel component of the structure yields $\Phi_{\parallel} = -0.6$ V, as shown in panel (b). Note that there is no net potential drop over the structure. The duration of the pulse is $\Delta t \sim 0.75$ msec, which gives a parallel scale length $L_{\parallel} \sim 300$ m. Under typical conditions at SLAMS, the Debye length is $\lambda_{\mathrm{D}} \sim 20$ m, thus $L_{\parallel} \sim 15\ \lambda_D$.

The analysis of 10 other SWs yields $v = 400$ - 1200 km/s, $L_{\parallel} \sim 300 - 600$ m and negative potentials of $|\Phi_{\parallel}| = 0.4 - 2.2V$, i.e., $e\Phi_{\parallel}/kT_e \sim O(0.1)$.

Figure 4 presents yet two more classes of signatures within SLAMS. Panels (a)-(b) show the signature of a tripolar structure with $\Delta t \sim 6$ msec and a peak-to-peak amplitude in the parallel electric field of $E'_{\parallel} \sim 55$ mV/m. Observations of similar structures have been reported in the literature (e.g., in the solar wind, see Mangeney et al., 1999). Panels (c)-(d) give an example of a large-amplitude ($E'_{\parallel} \sim 70$ mV/m) and high-frequency ($f \sim 630$ Hz) wave packet close to $f_{ce} \sim 640$ Hz. These wave packets are commonly observed in the IBM data within SLAMS. Most of the observed wave packets are close to $f_{ce} \sim 200 - 1500$ Hz, a few close to $f_{pi} \sim 1 - 2$ kHz.

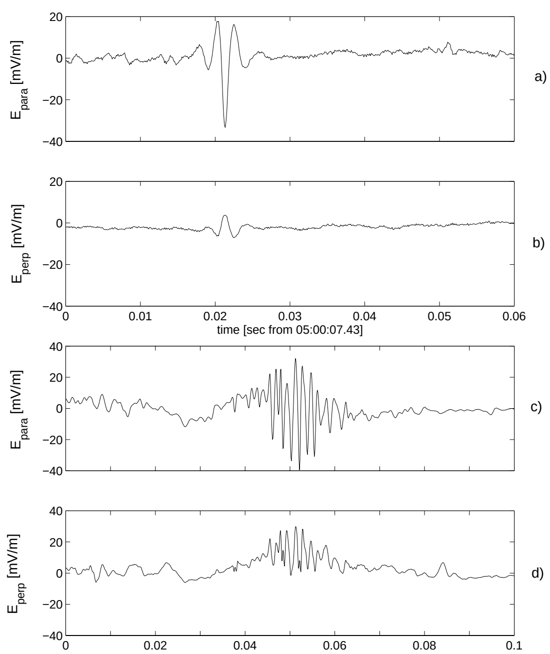

Figure 4. Panels (a)-(b) display $E_{\parallel}$ and $E_{\perp}$ for a tripolar solitary structure (spacecraft 2). Panels (c)-(d) show $E_{\parallel}$ and $E_{\perp}$ for a high-frequency wave packet (Cluster 4).

3. Discussion and Conclusions

We have reported on the first observations of nonlinear, electric field pulses (solitary waves, SWs) associated with Short Large-Amplitude Magnetic Structures (SLAMS) upstream of the Earth's quasi-parallel bow shock. Our measurements show together with earlier observations (see references in Sect. 1) that SWs are ubiquitous in naturally occurring plasmas containing currents.

The SWs move parallel to the background magnetic field with velocities of $v = 400$ - 1200 km/s and have peak-to-peak amplitudes in the parallel electric field of up to $E'_{\parallel} \sim 65$ mV/m. The parallel scale sizes are $L_{\parallel} \sim 300 - 400$ m $\sim O(10)\ \lambda_D$. The bipolar SWs exhibit negative potentials of $|\Phi_{\parallel}| = 0.4 - 2.2$ V, i.e., $e\Phi_{\parallel}/kT_e \sim O(0.1)$

In our study, the solar wind speed is ~ 400 km/s in the unshocked region before $\sim$ UT 04:50, whereas it reduces to ~ 200 km/s in the shock-like region after $\sim$ UT 04:50. Detailed particle data are not included in this study and simultaneous particle distribution functions for individual solitary waves can not be obtained with the present instruments. Using typical parameters for this region, we find thermal (about 10 eV) proton and electron speeds of about 50 and 2000 km/s, respectively.

An interesting question concerns the importance of SWs for the overall properties of SLAMS, including the importance for particle acceleration and for maintaining a larger scale parallel electric field. Most SWs have no obvious net potential drop. However, often a net potential of a few percent of $|\Phi_{\parallel}|$ can not be excluded since since other fluctuations with lower amplitude and longer duration are also present in the plasma. Comparing with other regions of space we note that McFadden et al. (2003) argue that ion phase space holes in the auroral region are a consequence of the acceleration process rather than maintaining the parallel potential drop. However, reports (e.g., Cattell et al., 2003) on electron solitary waves with $e\Phi_{\parallel}/kT_e \sim O(1)$ at the plasma sheet boundary suggest that these solitary waves might alter the electron distribution significantly. Again considering SWs in SLAMS, we can at this stage not conclude that the solitary structures are important for the main structure of the SLAMS.

A further issue is the association between SWs of different shapes, durations and scales. Observations with the Wideband (WBD) plasma investigation (Gurnett et al., 1997) onboard Cluster using one electric field component obtained at $\sim 2.2\ 10^5$ samples per second suggest another class of SWs within SLAMS. These SWs have durations of the order of 10's of microseconds (not shown here). Assuming the same velocity as for the SWs we study, this implies a scale size of the order of one Debye length. Similar structures observed in the magnetosheath have been interpreted as electron phase space holes (Pickett et al., 2003).

The knowledge of the speed and potential of our SWs in SLAMS allows us to discuss their nature. Firstly, the negative potential nature of the solitary waves would suggest that these are consistent with ion solitary waves. This would agree with the propagation of the slower moving structures with speeds around $v \sim 400$ km/s to be dominated by the convecting solar wind. The existence of SWs with higher velocities indicates the presence of other ion populations giving rise to different propagation speeds of the associated solitary structures. However, simulations (Barnes et al., 1985) suggest that ion solitary waves require a strongly magnetized plasma ($f_{\rm ce}/f_{\rm pe} \gg 1$) in order to grow. This is obviously not the case in the solar wind. Additionally, ion solitary waves have so previously only been observed for $f_{\rm ce}/f_{\rm pe} \gg 1$ (see references in Sect. 1). Secondly, electron phase space holes can be excluded as a possible interpretation, since these structures always are positive potential structures and move with a speed comparable to the thermal electron speed. Both conditions disagree with our observations. Thirdly, theoretical work (e.g., Mace and Hellberg, 2001) show that for most plasma models, electron acoustic solitary waves are negative potential structures. They do not require the plasma to be strongly magnetized, but propagate at speeds above the electron acoustic speed (Berthomier et al., 2000). This speed is above the speed of the thermal electrons, i.e. above about 2000 km/s. Hence, assuming typical particle distributions, electron acoustic solitary waves are not in agreement with the observed solitary waves. In conclusion we find that none of the theories commonly used to describe SWs are well suited to explain our observations. This shows the need to re-evaluate and improve simulations and theories concerning SWs.

Another example showing that present theories of SWs should be reconsidered and improved has recently been found at the quasi-perpendicular bow shock (Bale et al., 2002). Here electron holes have been observed convecting with the solar wind rather than moving with the much higher thermal electron speed.

A general question is how common and important SWs are in space plasmas. We have shown that SWs are common in SLAMS, as in several other regions with currents in and near the magnetosphere. Further studies are needed to determine the importance of SWs in SLAMS and in other regions. A fundamental question is how SWs in general can be described theoretically. We find that present theories must be improved to explain our observations, for example, by investigating if ion phase space holes may exist in weakly magnetized plasmas.

Acknowledgments. RB thanks A. Vaivads, A. Tjulin, A. I. Eriksson and S. C. Buchert for enlightening discussions. JSP acknowledges support from NASA GSFC Grant NAS5-9974.

References

Bale, S.D., et al., Electrostatic turbulence and Debye-scale structures associated with electron thermalization at collisionless shocks, *Ap. J., 575*, L25–L28, 2002.

Balogh, A., et al., The Cluster Magnetic Field Investigation: Overview of in-flight performance and initial results, *Ann. Geophys., 19*, 1207–1217, 2001.

Barnes, C., et al., Weak double layers in ion acoustic turbulence, *Phys. Fluids, 28*, 1055–1062, 1985.

Behlke, R., et al., Multi-point electric field measurements of Short Large-Amplitude Magnetic Structures (SLAMS) at the Earth's quasi-parallel bow shock, *Geophys. Res. Lett., 30*(4), 10.1029/2002GL015871, 2003.

Berthomier, M., et al., Electron-acoustic solitons in an electron-beam plasma system, *Phys. Plasmas, 7*, 2987–2994, 2000.

Boström, R., et al., G. Gustafsson, B. Holback, G. Holmgren, H. Koskinen, and P. Kintner, Characteristics of solitary waves and weak double layers in the magnetospheric plasma, *Phys. Rev. Lett., 61*, 82–85, 1988.

Bounds, S.R., et al., Solitary potential structures associated with ion and electron beams near 1 R_E altitude, *J. Geophys. Res., 104*, 28709, 1999.

Burgess, D., Cyclic behaviour at quasi-parallel collisionless shocks, *Geophys. Res. Lett., 16*, 345–348, 1989.

Cattell, C.A., et al., Observations of large amplitude parallel electric field wave packets at the plasma sheet boundary, *Geophys. Res. Lett., 26*, 857–860, 1998.

Cattell, C.A., et al., POLAR observations of solitary waves at high and low altitudes and comparison to theory, *Adv. Space Res., 28*, 1631–1641, 2001.

Cattell, C.A., et al., POLAR observations of solitary waves at the Earth's magnetopause, *Geophys. Res. Lett., 29*(5), 9:1–9:4, 10.1029/2001GL014046, 2002.

Cattell, C.A., et al., Large amplitude solitary waves in and near the Earth's magnetosphere, magnetopause and bow shock: Polar and Cluster observations, *Nonlin. Proc. Geophys., 10*, 13–26, 2003.

Crumley, J.P., et al., Studies of ion solitary waves using simulations including hydrogen and oxygen beams, *J. Geophys. Res., 106*, 6007–6015, 2001.

Dombeck, J., et al., Observed trends in auroral zone ion mode solitary wave structure characteristics using data from Polar, *J. Geophys. Res., 106*, 19013–19021, 2001.

Drake, J.F., et al., Formation of electron holes and particle energization during magnetic reconnection, *Science, 299*, 873–877, 2003.

Dubouloz, N., et al., Detailed analysis of broadband electrostatic noise in the dayside auroral zone, *J. Geophys. Res., 96*, 3565–3579, 1991.

Escoubet, C.P., et al., Cluster: Science and mission overview, *Space Sci. Rev. 79*, 11–32, 1997.

Gurnett, D.A., et al., The wide-band plasma wave investigation, *Space Sci. Rev., 79*, 195–208, 1997.

Gustafsson, G., et al., The Electric Field and Wave Experiment for the Cluster Mission, *Space Sci. Rev., 79*, 137–156, 1997.

Lucek, E.A., et al., Cluster magnetic field observations at a quasi-parallel bow shock, *Ann. Geophys., 20*, 1699–1710, 2002.

Mace, R.L., and M.A. Hellberg, The Korteweg-de Vries-Zakharov-Kuznetsov equation for electron-acoustic waves, *Phys. Plasmas, 8*, 2649–2656, 2001.

Mangeney, A., et al., WIND observations of coherent electrostatic waves in the solar wind, *Ann. Geophys., 17*, 307–320, 1999.

Matsumoto, H., et al., Electrostatic solitary waves (ESW) in the magnetotail: BEN wave forms observed by GEOTAIL, *Geophys. Res. Lett., 21*, 2915–2918, 1994.

McFadden, J.P., et al., FAST observations of ion solitary waves, *J. Geophys. Res., 108*(A4), 10.1029/2002JA009485, 2003.

Mozer, F.S., et al., New features of time domain electric-field structures in the auroral acceleration region, *Phys. Rev. Lett., 79*, 1281–1284, 1997.

Pedersen, A., et al., Four-point high time resolution information on electron densities by the electric field experiment (EFW) on Cluster, *Ann. Geophys., 19*, 1483–1489, 2001.

Pickett, J.S., et al., Solitary potential structures observed in the magnetosheath by the Cluster spacecraft, *Nonlin. Proc. Geophys., 10*, 3–11, 2003.

Schwartz, S.J., and Burgess, D., Quasi-parallel shocks: A patchwork of three-dimensional structures, *Geophys. Res. Lett., 18*, 373–376, 1991.

Schwartz, S.J., et al., Observations of Short Large-Amplitude Magnetic Structures at a quasi-parallel shock, *J. Geophys. Res., 97*, 4209–4227, 1992.

Temerin, M., et al., Observations of double layers and solitary waves in the auroral plasma, *Phys. Rev. Lett., 48*, 1175–1179, 1982.

R. Behlke, M. André, Swedish Institute of Space Physics, Uppsala division, Box 537, 75121 Uppsala, Sweden. (rico@irfu.se)

S.D. Bale, Space Science Laboratory, University of California, MC 7450, Berkeley, CA 94720, USA.

A. Balogh and E.A. Lucek, Blackett Laboratory, Imperial College, London, SW7 2BW, UK.

C.A. Cattell, School of Physics and Astronomy, University of Minnesota, 116 Church Street S.E., MN 55455 Minneapolis, USA.

J.S. Pickett, Department of Physics and Astronomy, University of Iowa, Iowa City, IA 52242, USA.